

SLAC-PUB-4678
October, 1988
(T/E)

LIGHT-CONE QUANTIZED QCD IN 1+1 DIMENSIONS*

KENT HORNBOSTEL

and

STANLEY J. BRODSKY

*Stanford Linear Accelerator Center
Stanford University, Stanford, California 94309*

HANS-CHRISTIAN PAULI

*Max Planck Institute for Nuclear Physics
D6900 Heidelberg 1, Germany*

ABSTRACT

The QCD light-cone Hamiltonian is diagonalized in a discrete momentum-space basis. The spectra and wavefunctions for various coupling constants, numbers of color, and baryon number are computed.

*Talk Presented to the Ohio State Workshop On
Relativistic Many-Body Physics, Columbus, Ohio, June 6-9, 1988*

* *Work supported by the Department of Energy, contract DE-AC03-76SF00515.

INTRODUCTION

Quantum Chromodynamics (QCD) potentially describes all of hadronic and nuclear physics in terms of quarks and gluons as fundamental degrees of freedom. Many features of the theory are consistent with experiment, especially at large momentum transfer where asymptotic freedom allows perturbative predictions. However, confrontation with the most significant and intrinsically non-perturbative aspects of the theory, its predictions for the spectrum and wavefunctions of hadrons, as well as the mechanisms for confinement and jet hadronization, still must wait for theoretical solutions. In this talk, the application to QCD in $1 + 1$ dimensions of a general non-perturbative approach to field theory ('Discretized Light-Cone Quantization (DLCQ)') developed in Ref. [1] is presented, and the prospects for $3 + 1$ dimensions are discussed.

$SU(N)$ gauge theories restricted to one spatial dimension and time have been studied extensively, both analytically^[2,3] and numerically,^[4,5] predominantly for the case when N is large. There are some special properties of these theories peculiar to $1 + 1$ dimensions which should be mentioned for the sake of orientation. Because there are no transverse directions, the gluons are not dynamical, and (in $A^+ = 0$ gauge) their presence is felt only by the constraint equation they leave behind. Likewise the quarks carry no spin. The fermion field may be represented as a two-component spinor, and chirality for massless fermions identifies only the direction of motion. The coupling constant g carries the dimension of mass, and for one quark flavor of mass m , the relevant parameter is g/m . After the subtraction of infinite constants, the theory is finite. Finally, the restriction to one spatial dimension produces confinement automatically, even for QED_{1+1} . The electric field is unable to spread out and the energy of a non-singlet state diverges as the length of the system.

In spite of these idiosyncracies, these models possess certain qualities to commend their study, not the least being tractability. There are only so many opportunities in a lifetime to solve, albeit numerically, a confining field theory with

arbitrary coupling from first principles. With solutions in hand, conceptual questions, points of principle, or approximation schemes which do not depend on the dimensionality of the model may be addressed. For example, Kröger has used QED_{1+1} quantized on the light-cone to discuss the numerical treatment of scattering for bound systems.^[6] Also, these models provide a test bed for approximation schemes and numerical techniques which may prove useful for realistic problems and a check on those, such as the large- N expansion, already in use. Ultimately, though, the motivation for this study is negative; if these models cannot be solved, there is no hope for QCD in $3 + 1$ dimensions.

LIGHT-CONE QUANTIZATION

Quantization on the light-cone is formally similar to standard canonical equal-time quantization, but with a few technical differences which nevertheless make life much easier. Given a (Lorentz-invariant) Lagrangian $\mathcal{L}(x^\mu)$, a new variable $x^+ \equiv x^0 + x^3$ is defined to play the role of time, along with new spatial variables (in four dimensions), $x^- \equiv x^0 - x^3$ and $x_\perp \equiv (x^1, x^2)$. Independent degrees of freedom are identified by the equations of motion. These are initialized to satisfy canonical commutation relations at $x^+ = 0$, and the creation and annihilation operators from their momentum space expansion define the Fock space. The momenta conjugate to x^- and x_\perp , P^+ and P_\perp respectively, are diagonal in this space and conserved by interactions. P^- acts as a Hamiltonian; in general it is complicated, dependent on the coupling constant, and it generates evolution in x^+ . Diagonalizing it is equivalent to solving the equations of motion.

The mass shell condition, $p^2 = m^2$, for individual quanta implies that $p^- = (m^2 + p_\perp^2)/p^+$, so that positive (light-cone) energy quanta must also carry positive p^+ . This seemingly innocent detail is actually a very good thing; the positivity of p^+ combined with its conservation is responsible in large part for the simplicity of this approach. First, x^+ -ordered perturbation theory becomes calculationaly viable because a large class of diagrams which appear in the time-ordered analog vanish.^[7] These include any diagram containing a vertex in which quanta are

created out of the vacuum; since all p^+ are positive, at such a vertex the total momentum cannot be conserved.

More importantly for the work described here, but by essentially the same reasoning, the perturbative vacuum is an eigenstate of the full, interacting Hamiltonian, with eigenvalue zero. Pairs of quanta cannot be produced which conserve p^+ .^[8] One very desirable feature of this remarkable fact is that not only is the ground state trivial, but also that all the quanta occurring in higher states are associated with meson and baryon wavefunctions rather than disconnected pieces of the vacuum.

Finally, it greatly simplifies the numerical work, especially in 1+1 dimensions.^[9] The system is quantized in a box of length L in the x^- direction with appropriate boundary conditions so that momenta are discrete and Fock space states denumerable. For the fixed total momentum P^+ , the relevant dimensionless momentum will be $K = \frac{L}{2\pi}P^+$. To see how K restricts the space of states, consider $K = 3$, which must be partitioned among the quanta in each state. The only three possibilities are (3), (2, 1), and (1, 1, 1). Contrast this with equal-time Fock states of definite P^+ . For equivalent numerical momentum, partitions will include not only those enumerated above, but also (4, -1), (104, -101), (5, 5, 3, 1, -1, -10), and so on. To keep the number of states finite, an additional cut-off in momentum must be introduced, whereas this is not necessary in the light-cone case.

Not only does a fixed K act implicitly as a momentum cut-off, it also severely limits both the total number of states of definite momentum and the number of quanta in each individual state, as the example above demonstrates. K serves one more role. The continuum limit $L \rightarrow \infty$ is equivalent to $K \rightarrow \infty$ as the physical momentum P^+ remains fixed. The size of K determines the physical size of the system, or equivalently, the fineness of the momentum space grid.

$SU(N)_{1+1}$ ^[10]

An $SU(N)$ gauge theory is defined by the Lagrangian

$$\mathcal{L} = -\frac{1}{4} F^{\mu\nu a} F_{\mu\nu}^a + \bar{\psi}(i\not{D} - m)\psi. \quad (1)$$

$F_{\mu\nu}^a$ is the field strength tensor $F_{\mu\nu}^a = \partial_\mu A_\nu^a - \partial_\nu A_\mu^a - gf^{abc}A_\mu^b A_\nu^c$ and the covariant derivative is defined as $iD_\mu = i\partial_\mu - gA_\mu^a T^a$. In two dimensions, the fermion field (in a representation in which γ^5 is diagonal)

$$\psi = \begin{pmatrix} \psi_L(x)_c \\ \psi_R(x)_c \end{pmatrix} \quad (2)$$

is a two-component spinor in the fundamental representation. L and R indicate chirality, which, for massless fermions specifies only direction.

A useful gauge choice is $A^+ = 0$. In this gauge there are neither ghosts nor negatively normed gauge bosons, so the Fock space quanta, and therefore the wavefunction constituents are physical and positively normed. Also, in 1+1 dimensions, this gauge choice is Lorentz (but not parity) invariant. The equations of motion are then

$$i\partial_- \psi_L = \frac{1}{2} m \psi_R \quad (3)$$

$$-\partial_-^2 A^{-a} = g\psi_R^\dagger T^a \psi_R \equiv \frac{1}{2} g j^{+a} \quad (4)$$

$$i\partial_+ \psi_R = \frac{1}{2} g A^{-a} T^a \psi_R + \frac{1}{2} m \psi_L \quad (5)$$

$$\partial_+ \partial_- A^{-a} = g\psi_L^\dagger T^a \psi_L - \frac{1}{2} g f^{abc} \partial_- A^{-b} A^{-c} \equiv \frac{1}{2} g j^{-a} \quad (6)$$

Only Eqs. (5) and (6) are dynamical; these will be generated by the Hamiltonian P^- . Eqs. (3) and (4) are constraints, as they involve only derivatives in x^- . At each time x^+ , both ψ_L and A^{-a} may be solved for in terms of ψ_R by inverting these derivatives with appropriate Green's functions.

ψ_R is evidently the only independent degree of freedom and as such is the only field quantized.^[11] The standard canonical commutator

$$\{\psi_R(x)_{c_1}, \psi_R(y)^{\dagger c_2}\}_{x^+=y^+} = \delta_{c_1}^{c_2} \delta(x^- - y^-) \quad (7)$$

may be implemented at $x^+ = 0$ by expanding in terms of creation and annihilation operators:

$$\psi_R(x^-)_c = \frac{1}{\sqrt{2L}} \sum_{n=\frac{1}{2}, \frac{3}{2}, \dots}^{\infty} \left(b_{n,c} e^{-i\frac{n\pi}{L}x^-} + d_{n,c}^{\dagger} e^{i\frac{n\pi}{L}x^-} \right). \quad (8)$$

The operators which generate translations in x^μ are derived from the energy momentum tensor:

$$P^\mu = \frac{1}{2} \int dx^- \Theta^{+\mu}. \quad (9)$$

P^+ , the momentum conjugate to x^- , is diagonal, $P^+ = \sum_n k_n^+ (b_n^{\dagger c} b_{n,c} + d_{n,c}^{\dagger} d_n^c)$, while P^- , which generates evolution in x^+ , is in general complicated and dependent on the coupling g . Diagonalizing P^- is equivalent to solving the equations of motion.

P^- in the space of color singlets may be divided into $P^- = m^2 H_0 + g^2 V$. $m^2 H_0$ is the free Hamiltonian which assigns an energy m^2/k^+ to each quark. The interacting piece is

$$g^2 V = -\frac{1}{4} \int dx^- dy^- |x^- - y^-| j^{+a}(x^-) j^{+a}(y^-), \quad (10)$$

where the current is normal-ordered: $j^{+a} = 2 : \psi_R^{\dagger} T^a \psi_R :$.

The potential $|x^- - y^-|$ is the result of inverting the constraint equation (4) for A^- . Finally, the interaction may be divided into a part V : which is entirely normal-ordered (Fig. 1b) and a remaining diagonal part V_{diag} (Fig. 1a) which contains a quark mass renormalization. The linear potential in position space

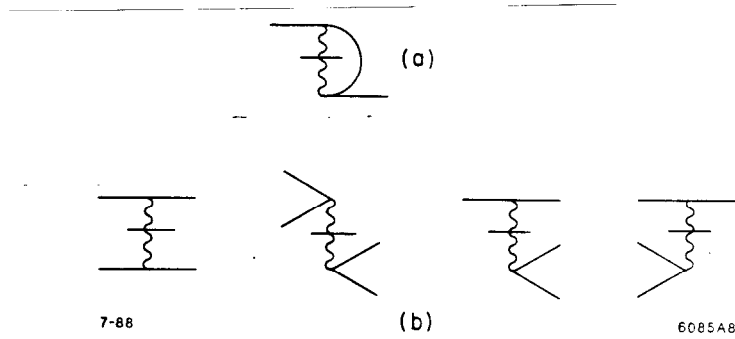


Figure 1. Interaction Vertices.

becomes the instantaneous gluon propagator $(1/p^+)^2$ in momentum space. Typical four-quark interactions in V have the form

$$\frac{L}{2\pi} \frac{g^2}{\pi} \frac{1}{2} (\delta_{c_4}^{c_2} \delta_{c_1}^{c_3} - \delta_{c_4}^{c_3} \delta_{c_1}^{c_2}) \sum_{n_i = \frac{1}{2}, \frac{3}{2}, \dots} \frac{\delta_{n_1+n_2, n_3+n_4}}{(n_1+n_3)^2} b_{n_4}^{\dagger c_4} b_{n_3, c_3} d_{n_2, c_2}^{\dagger} d_{n_1}^{c_1}. \quad (11)$$

THE PROGRAM

In order to evaluate and diagonalize P^- numerically, the system is quantized in a box in x^- of length $2L$ and boundary conditions are selected. Consequently, the momenta are discrete, denumerable and therefore digestible by the computer. To expand ψ_R in a complete set of plane-wave solutions of the free equations of motion, anti-periodic boundary conditions are employed. (For periodic conditions the term with $k^+ = 0$, needed for completeness, is not a solution of the free equation $k^+k^- = m^2$ except when m is zero.) The field ψ_R expanded in operators with discrete momenta is then inserted in Eq. (9) to produce the discretized Hamiltonian P^- .

The program is set up to run for arbitrary number of colors N , baryon number B , and numerical momentum $K = (L/2\pi)P^+$. Given these, it constructs the Fock space by generating all possible distributions of K among quarks in color singlets. In general, this construction is over-complete. The inner product matrix $\langle i|j \rangle$ of

these states is evaluated and diagonalized; redundant states are identified by zero eigenvalues and removed; those remaining are orthonormal and complete.

The Hamiltonian matrix $\langle i|H|j\rangle$ is evaluated in this basis, with the color contractions performed diagrammatically. Because the light-cone Hamiltonian breaks up simply into H_0 proportional to m^2 and V to g^2 , the corresponding matrices are stored separately. Altering g (or m) involves only multiplying these matrices by the new parameter prior to diagonalization, with almost no additional cost in time.^[12]

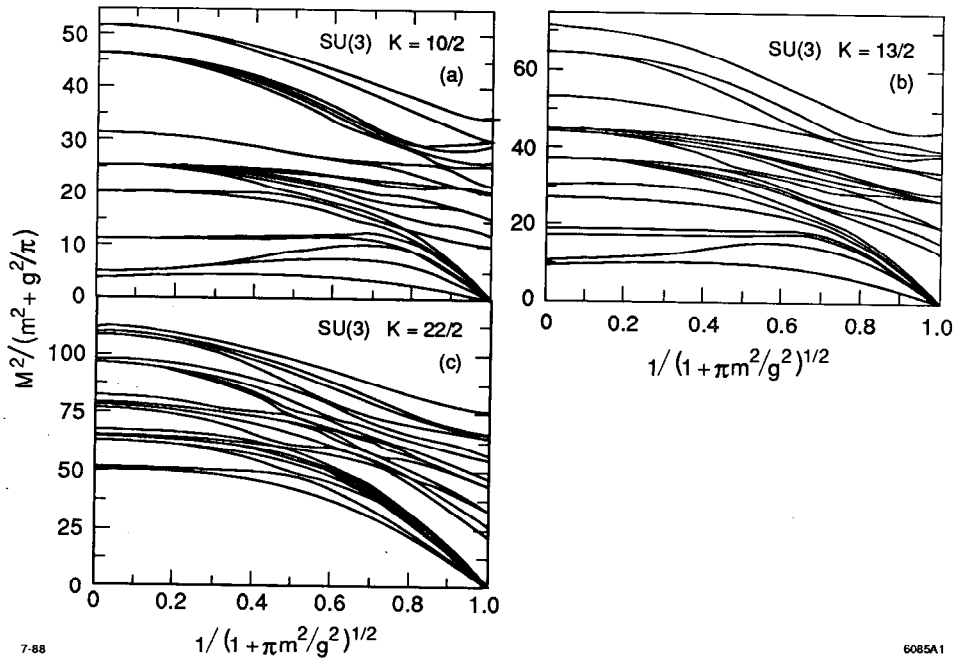


Figure 2. Spectra for $N = 3$, baryon number $B = 0, 1$ and 2 as a function of g/m ; K fixed.

Setting g/m , combining H_0 and V , and diagonalizing produces the full spectrum (Fig. 2). Included in the spectra are not only single mesons and baryons and their excited states, but also multiple-hadron scattering states. Note the large number of massless mesons and baryons in the strong coupling (small mass) limit.

WAVEFUNCTIONS

Diagonalization gives not only eigenvalues but also their eigenvectors, or wavefunctions. Because the perturbative vacuum is also the full interacting vacuum, all quanta in the wavefunctions are associated with mesons and baryons, making them simple to interpret and straightforward to employ in calculations.^[13] Expressed in terms of the Bjorken variable $x \equiv k^+/P_{total}^+$, they are invariant under longitudinal Lorentz boosts, and so, in $1 + 1$ are Lorentz-invariant. Parity is more complicated, as it is not respected by the quantization scheme. For wavefunctions with two particles in $1 + 1$, however, it involves only an interchange of x variables.

Finally, these wavefunctions are universal; they contain all of the information about the hadrons. Once computed, masses, form factors and inclusive and exclusive scattering amplitudes are reduced to computing a few integrals. For example, in four dimensions, the ratio

$$R(Q^2) = (\sigma_{e^+e^- \rightarrow hadrons} / \sigma_{\mu^+\mu^- \rightarrow hadrons}) \quad (12)$$

is a textbook example of a quantity calculable in QCD when Q^2 is large. The relevant matrix element, $(e^2/Q^2) \bar{v}\gamma_\mu u \langle hadrons | J_{em}^\mu | 0 \rangle$ is typically squared and related to vacuum polarization graphs, which are then computed as an expansion in $\alpha_s(Q^2)$. However, were someone to provide the appropriate hadronic wavefunctions, this matrix element could be computed directly at any Q^2 . A feature such as the ρ resonance would then appear as an enhancement in the density of states in the $\pi\pi$ continuum.

The valence wavefunctions for the lightest $N = 3$ meson and baryon are displayed in Fig. 3 by means of their quark structure functions. For weak coupling ($m/g = 1.6$) the quark mass dominates p^+ and so momentum peaks around equal sharing among constituents ($x = \frac{1}{2}$ and $\frac{1}{N}$ for the meson and baryon, respectively). Stronger coupling tends to smear out the distribution.

Wavefunctions contain in general higher Fock components with additional numbers of quarks. Figs. 4a and b illustrate the contribution to the quark structure

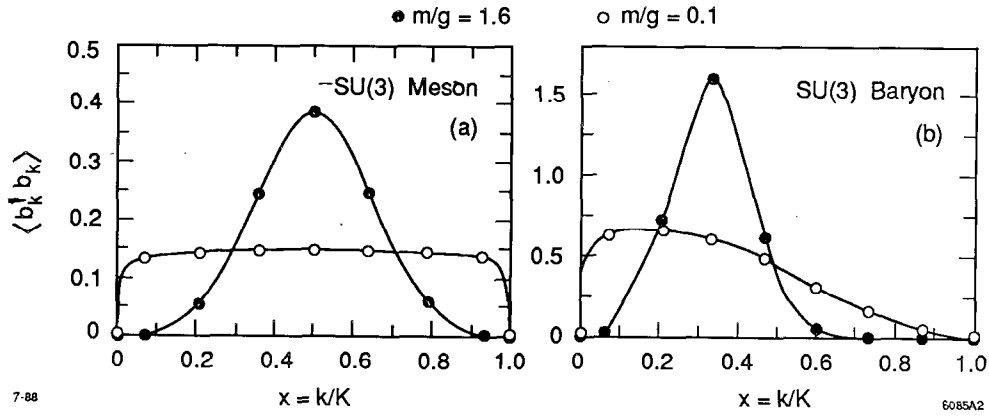


Figure 3. Valence structure functions for $N = 3$ baryon and meson at $m/g = 0.1$ and 1.6 .

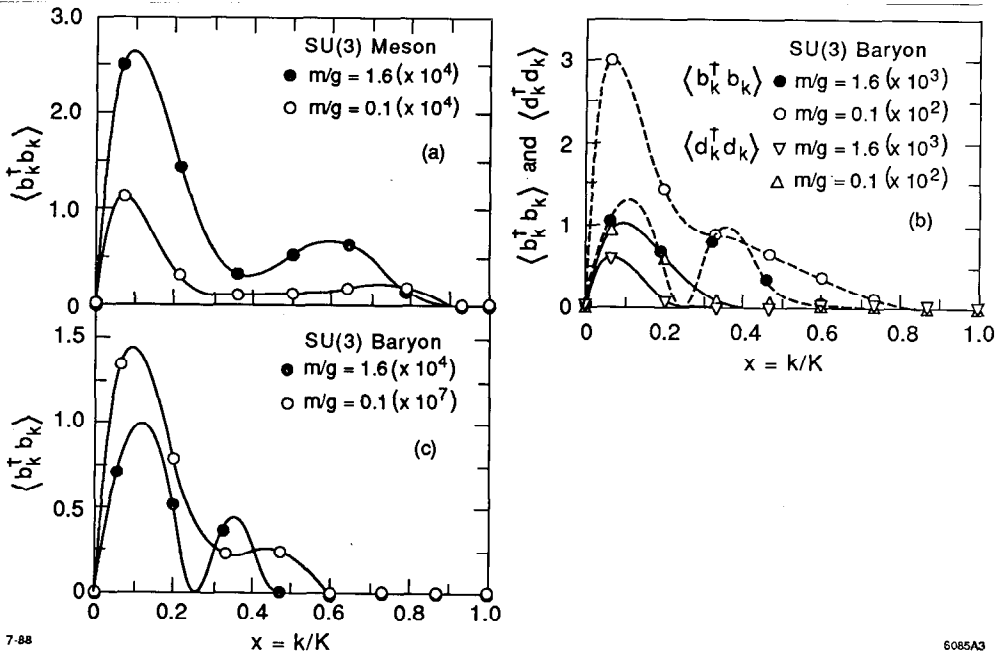


Figure 4. Higher Fock contributions to $N = 3$ structure functions. a) Lightest meson. b) Lightest baryon, including antiquarks. c) Baryon: contribution from two extra quark pairs.

function from the component of the lightest $N = 3$ meson and baryon wavefunction with an additional $q\bar{q}$ pair. Their contribution is suppressed relative to that of the valence wavefunction by from two to four orders of magnitude. Because P^+ must be distributed among more quanta, the average x is lower. The characteristic bump structure may be understood in terms of $q\bar{q}$ pairs splitting off of the valence quarks, at least for weak coupling.^[14] Fig. 4b also includes the antiquark structure functions and gives an indication of the pion content of the baryon. Fig.

4c presents the (negligible) contribution from the Fock state with two extra quark pairs.

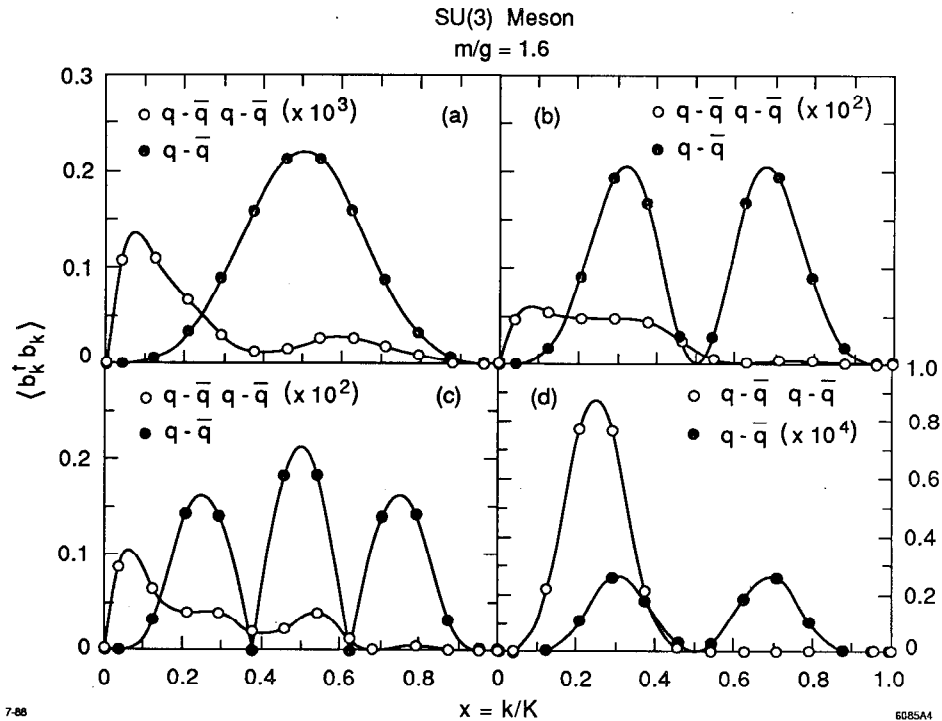


Figure 5. a-c) First three states in $N = 3$ meson spectrum for $m/g = 1.6$, $2K=24$. d) Eleventh state.

Of course the spectrum consists of many states beyond the lightest. Because the quanta are associated only with the hadron, the wavefunctions need not be disentangled from the vacuum and are often relatively simple to interpret. In Fig. 5, the first three (weakly coupled) meson wavefunctions are clearly the first three radial excitations of a predominantly $q\bar{q}$ state. In fact, in the non-relativistic limit these become the momentum transforms of Airy functions.^[15] In Fig. 5d the dominant contribution is from two $q\bar{q}$ pairs peaked at $x = 1/4$, with a mass twice that of the first state; it clearly represents a pair of the lightest mesons. Fig. 6 presents a similar picture for the $N = 3$ baryons. The pair of baryons in Fig. 6d is selected from the $B = 2$ spectrum. For strong coupling, it is more difficult to

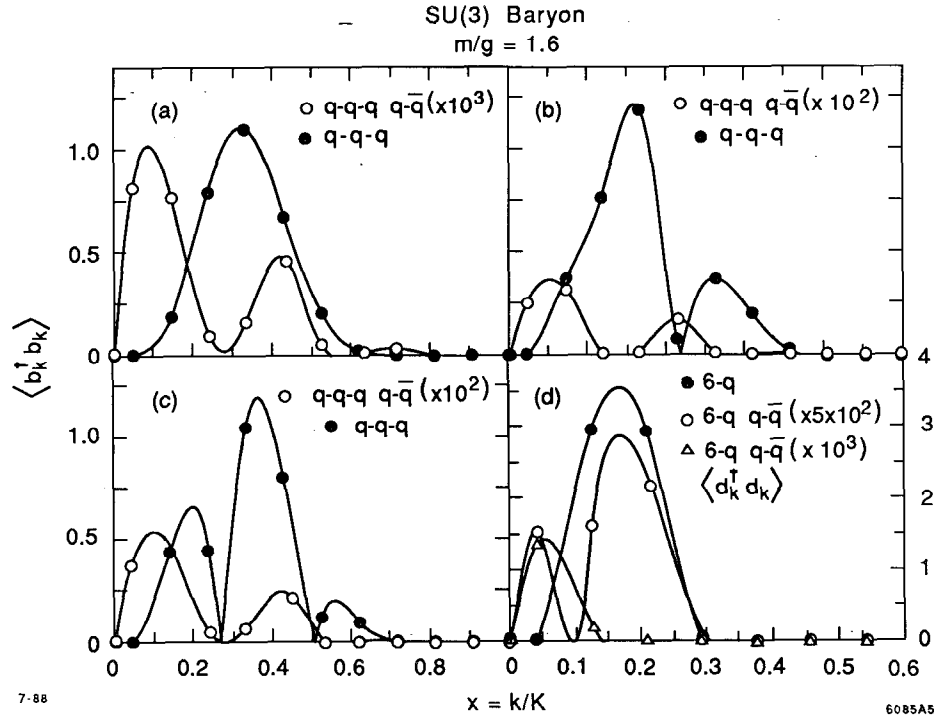


Figure 6. a-c) First three states in $N = 3$ baryon spectrum, $2K=21$. d) First $B = 2$ state.

disentangle states due to the presence of a large number of very light mesons and baryons.

MASSLESS MESONS AND BARYONS IN THE $m/g \rightarrow 0$ LIMIT

The massless hadrons at zero quark mass may be understood by studying the momentum space transforms of the $SU(N)$ currents (at $x^+ = 0$)

$$V_k^a = \frac{1}{2} \int_{-L}^L dx^- e^{-i\frac{k\pi}{L}x^-} j^{+a}(x^-) \quad (13)$$

which satisfy $[V_k^a, V_l^b] = if^{abc}V_{k+l}^c + \frac{1}{2}l\delta^{ab}\delta_{k+l,0}$. The currents j^{+a} are defined by point splitting along x^- ; for $A^+ = 0$, the path-ordered exponential included to ensure gauge invariance reduces to one. The algebra may be extended to include the $U(1)$ current $j^+ = (\frac{2}{N})^{\frac{1}{2}} : \psi_R^\dagger \psi_R :$. The transformed operator V_k commutes

with the other $SU(N)$ elements, and the related operator $a_k^\dagger \equiv \left(\frac{2}{k}\right)^{\frac{1}{2}} \epsilon(k) V_k$ satisfies the free boson commutation relations $[a_k, a_k^\dagger] = \delta_{k,l}$.

The interacting part of the Hamiltonian is greatly simplified when expressed in terms of these operators:

$$P_I^- = -\frac{g^2}{16} \int_{-L}^L dx^- dy^- |x^- - y^-| j^{+a}(x^-) j^{+a}(y^-) \quad (14)$$

becomes

$$\frac{L}{2\pi} \frac{g^2}{2\pi} \sum_{k=-\infty}^{\infty} \frac{1}{k^2} V_k^a V_{-k}^a. \quad (15)$$

Because $V_0^a = Q^a$, the contribution at $k = 0$ is proportional to the total charge $Q^a Q^a$ and so may be discarded.

The V_k are color-singlet bilinears in ψ_R , and so may be used to create mesonic-like states with momentum $P^+ = \frac{2\pi k}{L}$. In the limit where m/g is zero, the entire Hamiltonian is given by Eq. (15). Because the V_k commute with the V_k^a which appear in P_I^- ,

$$M^2 V_k |0\rangle = \frac{2\pi k}{L} [P^-, V_k] |0\rangle = 0. \quad (16)$$

Not only is the state created by acting with V_k on the vacuum an exactly massless eigenstate in this limit, but states formed by repeated applications are also exactly massless. Furthermore, acting with V_k on an eigenstate of non-zero mass produces a degenerate state of opposite parity. This argument is independent of the value of the numerical momentum K and so gives an exact continuum result.

Just as the existence and number of massless states is most simply discussed in terms of the V_K , so also are the wavefunctions of these states. Applying one V_K to the vacuum

$$V_K |0\rangle = \frac{1}{\sqrt{2N}} \sum_{n=\frac{1}{2}, \frac{3}{2}, \dots}^{K-\frac{1}{2}} b_{K-n}^{\dagger c} d_{n,c}^\dagger |0\rangle \quad (17)$$

yields a continuum wavefunction of $\phi(x) = 1$ (where $n/2K \rightarrow x$). Because ϕ is

even under the interchange of x and $1 - x$, this state is a pseudoscalar. The wavefunctions of momentum K created by applying V twice are, for any $l < K$,

$$V_{K-l} V_l |0\rangle = \frac{1}{2N} \left[\sum_{n=\frac{1}{2}}^{l-\frac{1}{2}} \left(b_{K-n}^{\dagger c} d_{n,c}^{\dagger} - b_n^{\dagger c} d_{K-n,c}^{\dagger} \right) + \sum_{m=\frac{1}{2}}^{K-l-\frac{1}{2}} \sum_{n=\frac{1}{2}}^{l-\frac{1}{2}} b_{K-l+m}^{\dagger c_2} d_{m,c_2}^{\dagger} b_{l-n}^{\dagger c_1} d_{n,c_1}^{\dagger} \right] |0\rangle. \quad (18)$$

The $q\bar{q}$ piece is odd; therefore this state is a scalar, as a product of pseudoscalars must be. All the massless meson wavefunctions for a given K may be constructed in this manner; parity will alternate with each additional V .

Were the gauge group $U(N)$ rather than $SU(N)$ ^[16] the additional term associated with the extra $U(1)$,

$$\frac{L}{2\pi} \frac{g^2}{2\pi} \sum_{k=1}^{\infty} \frac{1}{k} a_k^{\dagger} a_k, \quad (19)$$

appears in P^- . The a_k satisfy free bosonic commutation relations, and this additional interaction is therefore the discrete light-cone Hamiltonian for free bosons of mass squared $g^2/2\pi$. These formerly massless states created by the a_k^{\dagger} are promoted to the free massive bosons found in the Schwinger model and discussed in [17] and [18]. The wavefunctions for these states however are unchanged.

Note that while the entire $U(1)$ spectrum may be built up from these non-interacting bosons,^[18] for $U(N)$ or $SU(N)$ they describe only part of the spectrum; these are the massless mesons for $SU(N)$. In addition there are massive states which include excited $q\bar{q}$ pairs.

Similarly, the composite baryon field

$$B_k \equiv \frac{1}{2} \int_{-L}^L dx^- e^{-i\frac{k\pi}{L}x^-} \epsilon_{c_1 \dots c_N} \psi_R^{\dagger c_1}(x^-) \dots \psi_R^{\dagger c_N}(x^-) \quad (20)$$

commutes with the V_k^a , and, in the limit $m/g \rightarrow 0$, with the Hamiltonian P^- . As in the case for mesons, this field creates an identically massless baryon. Repeated applications on the vacuum produce a massless state with arbitrarily desired baryon number. Furthermore, degenerate states with the same baryon number may be created by acting with the massless mesonic operators V_k in conjunction with the B_k . Again, these results are independent of K and are true in the continuum limit. The (unnormalized) wavefunction associated with this massless baryon is

$$B_k |0\rangle = \frac{1}{2(2L)^{\frac{N-1}{2}}} \sum_{n_i} \delta_{K, \Sigma n_i} \epsilon_{c_1 \dots c_N} b_{n_1}^{\dagger c_1} \dots b_{n_N}^{\dagger c_N} |0\rangle. \quad (21)$$

Whether this state is a fermion or boson depends on N being odd or even. The quark distribution derived from this wavefunction for $N = 3$ becomes $6(1 - x)$ in the continuum limit; this x dependence is clearly evident in Fig. [3]. The general expression for the quark distribution for a single baryon in the $m/g \rightarrow 0$ limit is

$$q(x) = N(N - 1)(1 - x)^{N-2}. \quad (22)$$

For $N = 2$, $q(x) = 2$, which apart from the normalization, is identical to the meson distribution for all N .

NUMERICAL ACCURACY

A great deal of information about solutions in the continuum limit may be extracted by restricting the Fock space to a single $q\bar{q}$ pair. This is a good approximation to the lightest meson and its radial excitations, but neglects a large part of the low-lying spectrum when g/m is large.

Restricting the eigenvalue equation

$$M^2 |\phi(P^+)\rangle = P^- P^+ |\phi(P^+)\rangle \quad (23)$$

to the $q\bar{q}$ subspace and taking the limit $K \rightarrow \infty$ yields the integral equation^[19]

$$M^2\phi(x) = m^2 \left(\frac{1}{x} + \frac{1}{1-x} \right) \phi(x) - \frac{g^2}{\pi} \left(\frac{N^2 - \alpha}{2N} \right) P \int_0^1 dy \frac{\phi(y) - \phi(x)}{(y-x)^2} \\ + \frac{g^2}{\pi} \left(\frac{(1-\alpha)N}{N} \right) \int_0^1 dy \phi(y). \quad (24)$$

For $SU(N)$, $\alpha = 1$, and $\alpha = 0$ for $U(N)$. The continuum wavefunction $\phi(x)$ is defined by

$$|\phi(P^+)\rangle = \int_0^1 \frac{dx}{[4\pi Nx(1-x)]^{\frac{1}{2}}} \phi(x) b_{(1-x)P^+}^{\dagger c} d_{xP^+,c}^{\dagger} |0\rangle. \quad (25)$$

This equation incorporates all of the leading order dynamics of the large- N approximation.^[2] Because it could be derived from the discretized Hamiltonian in the continuum limit $K \rightarrow \infty$, it demonstrates that this limit is sensible. Also, it shows trivially that, when $m = 0$, $\phi(x) = 1$ is an eigenfunction with $M^2 = 0$ for $SU(N)$, $g^2/2\pi$ for $U(N)$. The latter is the well-known Schwinger Model boson.

More importantly for this work, it shows the error due to discretization as that of an integral evaluated numerically on a regularly spaced grid, with spacing $\epsilon = 1/K$. This is not normally the most efficient method, and this case is not even normal. In addition to the typical errors of order ϵ^n , $n \geq 2$, the principal-value-regulated singularity in Eq. (24) induces an error of order ϵ . Also, for small x , $\phi(x) \propto x^a$, with a given implicitly by^[2]

$$1 - a\pi \cot(a\pi) = \frac{\pi m^2}{g^2 \left(\frac{N^2 - 1}{2N} \right)}; \quad (26)$$

a ranges from zero (when $m/g = 0$) to one ($g/m = 0$). This non-analytic endpoint behavior produces additional a -dependent errors. As a result, a mass, for example

measured at finite K behaves as

$$M\left(\frac{1}{K}\right) = M(0) + \frac{c_1}{K} + \frac{c_2}{K^{1+a}} + \frac{c_3}{K^2} + \frac{c_4}{K^{2+a}} + \dots; \quad (27)$$

$M(0)$ is the continuum limit. This behavior, as well as Eq. (26) apply as well to baryons and higher Fock states.^[10] Knowing Eq. (27), convergence may be improved significantly by Richardson extrapolation: compute M at n different K , and fit to Eq. (27). An estimate of the error in determining $M(0)$ is given by the n^{th} term.

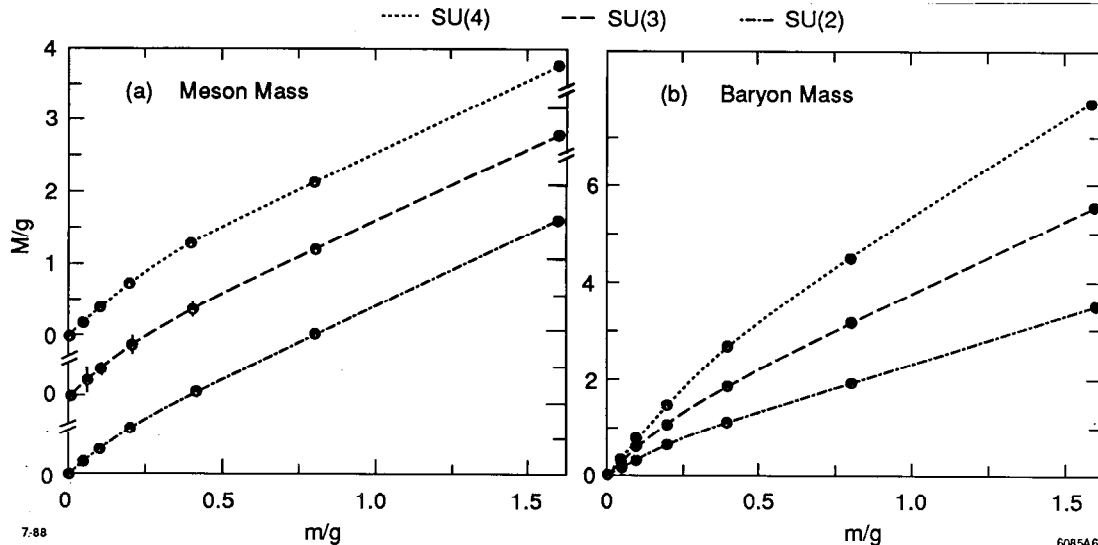


Figure 7. Extrapolated masses for $N = 2, 3$ and 4 meson and baryon.

This extrapolation has allowed for meaningful numerical results from the relatively low $K \approx 10$, as well as error estimates. Plots for the lightest meson and baryon for $N = 2, 3$ and 4 are presented in Fig. 7; when not visible, the estimated error bars are smaller than the data point. The zero masses at $m/g = 0$ are exact. The next two at $m/g = .05$ and $.1$ are probably not close enough to convergence for the assigned errors to be more than rough estimates.

Finally, these data may be compared with previous calculations. Fig. 8b demonstrates the rapid meson mass approach to the large- N limit from Ref. [2] as N increases from two to four. In Fig. 8a, points from the Hamiltonian lattice calculation^[4] of Hamer for $N = 2$ agree well with the light-cone results. This is

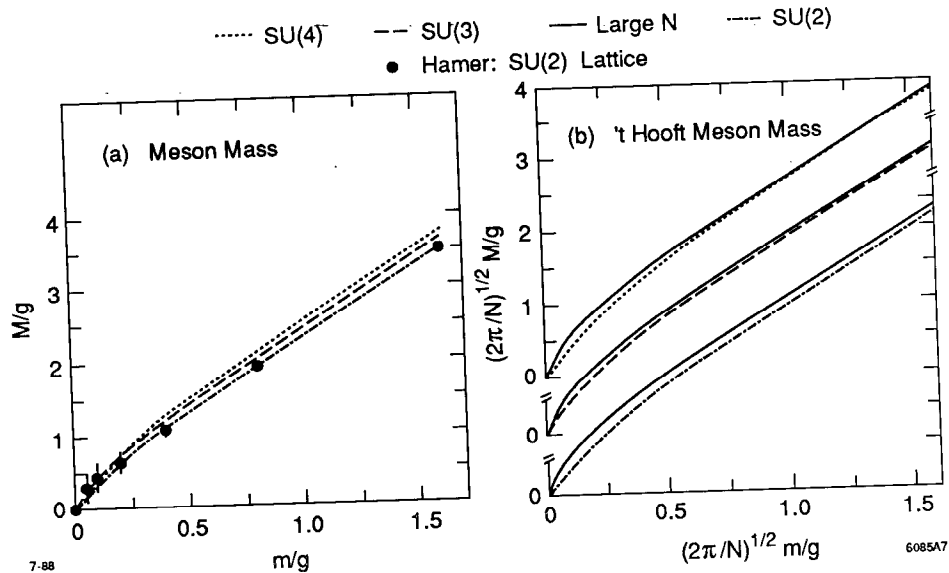


Figure 8. Comparison of $N = 2, 3$ and 4 meson masses with large- N and lattice calculations.

gratifying in that, while both techniques possess peculiarities, they are peculiar in different places. Also, the ratio of lightest meson to baryon masses in the strong-coupling limit for $N = 2, 3$ and 4 , are consistent (to within the roughly 10% error) with the ratio $2 \sin(\frac{\pi}{2(2N-1)})$ derived by bosonization.^[20]

LARGE- N APPROXIMATION

Most previous work on this model employed the large- N approximation to leading order. By obtaining numerical solutions at finite N , the validity of this approximation for interesting values of N (three, for example) can be tested. From Figs. 7 and 8, for weak coupling (large quark mass) it is quite good. The meson mass is already well approximated for $N = 2$, and, as expected, the baryon masses increase proportionally with N . The low-lying states are indeed $q\bar{q}$ excitations; higher Fock contributions are negligible. For strong coupling (small mass), the approximation is not as reliable; the effective expansion parameter $g^2 N/m^2$ is no longer small. Light baryons exist for all finite N and so may not be neglected. The low-lying meson spectrum is dominated by states with arbitrary numbers of quarks rather than $q\bar{q}$ excitations. Finally, the $U(N)$ meson mass (as $m/g \rightarrow 0$) of $g^2/2\pi$ is neglected in the large- N limit.

PROSPECTS IN FOUR DIMENSIONS

QCD in two dimensions is both manageable and instructive, but the world in reality consists of (at least) four. Not surprisingly, the problem becomes much more challenging, as introducing transverse directions greatly increases the degrees of freedom. Spin for the quarks, and (in $A^+ = 0$ gauge) physical, transversely polarized gluons must be included, and both carry transverse momentum, which may be discretized on a Cartesian grid, $p_{\perp}^i = (2\pi/L_{\perp})n_{\perp}^i$. The n_{\perp}^i can be negative, and will be restricted by the cut-off discussed below. As the Fock space grows roughly exponentially with the degrees of freedom, exploiting the remaining symmetries of the light-cone Hamiltonian under, for example, isospin, charge conjugation, and rotations of 90° in the transverse plane will be necessary to restrict the space.

In contrast to $1+1$ dimensions, QCD_{3+1} requires a non-trivial renormalization. This may be implemented directly on the space of states by restricting it to those whose invariant mass satisfies

$$M^2 = \sum \frac{k_{\perp}^2 + m^2}{x} < \Lambda^2. \quad (28)$$

The cut-off Λ must be sufficiently larger than the scale of interest, with physics beyond it absorbed into the couplings and masses.^[13] As is, this prescription is Lorentz, but not gauge, invariant, and likely will need to be improved. Finally, gauge invariance may be checked by showing, for example, that in the continuum and large- Λ limits matrix elements such as $q_{\mu} \langle 0 | j^{\mu} | q \rangle$ vanish, and, for QED , that the photon remains massless.

A crude estimate of the difficulty of this problem may be made by selecting minimum appropriate values for Λ of 1 GeV and 1 fermi for $(L_{\perp}/2\pi)$. These correspond, by Eq. (28), to $x \sim 1/K \sim 1/25$ and $n_{\perp} \sim 5$. This allows some hope that systems with longitudinal momentum K comparable to that used in $1+1$ dimensions combined with the first several transverse modes may begin to provide a recognizable picture of hadronic physics.

Presently, programs for QED_{3+1} have been written by A. Tang and H. C. Pauli and are under investigation. Among other things, positronium will be studied for various couplings. Initial attacks on QCD_{3+1} will most likely involve purely gluonic or heavy $q\bar{q}$ systems.

ACKNOWLEDGEMENTS

K. H. would like to thank the organizers for the privilege of participating in this conference. S. J. B. and H. C. P. thank A. Tang, M. Kaluza, and T. Eller for helpful conversations. S.J.B. wishes to acknowledge the support of the Alexander von Humboldt Foundation and the hospitality of the Max-Planck Institute for Nuclear Physics, Heidelberg.

REFERENCES

1. Pauli, H. C., and Brodsky, S. J., Phys. Rev. **D32**, 1993 (1985); **D32**, 2001 (1985).
2. 't Hooft, G., Nucl. Phys. **B75**, 461 (1974).
3. Callan, C. G., Coote, N., and Gross, D. J., Phys. Rev. **D13**, 1649 (1976).
Einhorn, M. B., Phys. Rev. **D14**, 3451 (1976). Bars, I., and Green, M. B.,
Phys. Rev. **D17**, 537 (1978).
4. Hamer, C. J., Nucl. Phys. **B195**, 503 (1982).
5. Huang, S., Negele, J. W., and Polonyi, J., MIT preprint MIT-CTP-1545.
6. Kröger, H., these proceedings.
7. Weinberg, S., Phys. Rev. **150**, 1313 (1966).
8. This is certainly not the last word on this subject, though it will be the last one here. For instance, this is not strictly true if there are quanta for which p^+ is zero. See for example Harindranath, A., and Vary, J., Phys. Rev. **D37**, 3010 (1988). There are other subtleties which will be addressed in future work.

9. Pauli, H. C., and Brodsky, S. J., Phys. Rev. **D32**, 1993; **D32**, 2001 (1988).
10. Hornbostel, K., Ph.D. thesis; to appear as a SLAC Report.
11. For an introduction to light-cone quantization, cf. Yan, T.-M., Phys. Rev. **D7**, 1780 (1972) and references therein.
12. Typical cases presented here required one to three minutes of CPU on an IBM 3081.
13. For a general review of wavefunctions in QCD, cf. Lepage, G. P., Brodsky, S. J., Huang, T., and Mackenzie, P. B., CLNS-82/522, published in Banff Summer Institute 81 (1981). Lepage, G. P., Brodsky, S. J., Phys. Rev. **D22**, 2157 (1980).
14. Blankenbecler, R., private communication.
15. Hamer, C. J., Nucl. Phys. **B121**, 159 (1977); **B132**, 542 (1978).
16. This is the group considered by 't Hooft, Ref. [2]. The two are equivalent in the large- N limit. In general the extra $U(1)$ introduced need not be associated with the same coupling constant as $SU(N)$, but this is sufficient for this discussion.
17. Bergknoff, H., Nucl. Phys. **B122**, 215 (1977).
18. Eller, T., Pauli, H. C., and Brodsky, S. J., Phys. Rev. **D35**, 1493 (1987).
19. Eller, T., thesis; unpublished.
20. Date, G. D., Frishman, Y., and Sonnenschein, J., Nucl. Phys. **B283**, 365 (1987), and Sonnenschein, J., private communication.